

THESIS FOR THE DEGREE OF DOCTOR OF PHILOSOPHY (PHD)

**The formation and decomposition kinetics of  
*N*-chloro amino acids**

Mária Szabó

Supervisor: Dr. István Fábián professor



UNIVERSITY OF DEBRECEN  
DOCTORAL SCHOOL OF CHEMISTRY

DEBRECEN, 2019



## Introduction and objectives

In recent years, the reactions of chlorine and hypochlorous acid with amines, amino acids and peptides have been the subject of intensive research due to their relevance in environmental chemistry, and *in vivo* processes. Depending on the conditions, these reactions lead to the formation of a wide variety of *N*-chloramines. Various amino compounds can react with chlorine or hypochlorous acid in chlorination wastewater and drinking water treatment technologies. *N*-chloro amino acids are secondary disinfectants, because they are involved in the destruction of microorganisms. Environmental concerns have generated immense interest in the chemistry of these compounds and the products of their decomposition.

The same reactions are also important in biological systems. During inflammatory processes in the body, hypochlorous acid is formed in the myeloperoxidase enzyme catalyzed reaction between chloride ion and hydrogen peroxide. In subsequent oxidation processes, hypochlorous acid chlorinates amino acids and related compounds in a few seconds. *N*-chloro amino acids are unstable on a longer timescale, and their decomposition yields various intermediates and products. While these compounds play an important role in the defense mechanism against pathogens, they also have adversary biological effects. The biological activity of *N*-chloro amino acids is due to their ability to penetrate into the cell. Inside the cell, they induce oxidative stress which leads to apoptosis or necrosis. Beside the pathogens, healthy cells are also killed in this process. In addition, *N*-chloro amino acids may have indirect cytotoxic and/or genotoxic effects caused by the intermediates and products of their degradation.

The chemistry and biological role of *N*-chloro amino acids have been studied in detail, but many questions remained unanswered and some of the results are highly controversial. Therefore, our aim was to answer these questions, to gain a

deeper understanding of the kinetics and mechanism of the formation and degradation reactions of these compounds, and to clarify the contradictions.

## **Instrumentation and computational methods**

Iodometric and pH-metric titrations were performed with a Metrohm 888 titrator, to which a Metrohm Platinum 6.0451.100 Platinum or a Metrohm 6.0262.100 combined glass electrode was attached.

The acid dissociation constants of the amino acids were determined by pH-metric titration, and the experimental data were evaluated using the SUPERQUAD software.

In order to investigate the formation of *N*-chloro amino acids, an Applied Photophysics SX-20 stopped-flow device was used which was equipped with a photoelectron multiplier detector. Kinetic curves were recorded using 10.0 mm optical path length. A single kinetic curve was obtained as the average of 3 to 5 replicate kinetic runs. First-order kinetic curves were evaluated with the controlling software of the instrument. All other data fittings were performed with OriginPro 2018 using a non-linear least squares routine.

Decomposition kinetic studies were performed with an Agilent Technologies Cary 8454 UV-Vis diode array spectrophotometer. Measurements were made in a closed tandem cuvette with a light path of 8.74 mm. The cell temperature was kept constant with the Peltier-type thermostat built into the device.

NMR measurements were performed on a Bruker DRX 400 (9.4 T) spectrometer equipped with a Bruker VT-1000 temperature controller and a BB inverted gradient head (5 mm). Since NMR measurements were carried out with aqueous solutions, a water suppression technique was used. The signal of the protons of water (4.8 ppm) was eliminated with a watergate pulse sequence (12.6 dB). A sealed capillary containing DSS (4,4-dimethyl-4-silapentane-1-sulfonic

acid) dissolved in D<sub>2</sub>O was also placed in the NMR tubes. DSS served as an external standard for determining the chemical shift of <sup>1</sup>H NMR signals. For the <sup>1</sup>H NMR spectra, 32 scans were made in one experiment with an acquisition time of 1.366 s. Spectra were analyzed with Bruker WinNMR and MestReNova software packages. J-modulated <sup>13</sup>C NMR spectra were recorded in a 22075 Hz window with 0.74 s acquisition time and 5 s relaxation time. Standard Bruker pulse programs were used for COSY, NOESY, HSQC and HMBC experiments.

Mass spectra were recorded in positive and negative ion modes on a Bruker micrOTOF-Q type Qq-TOF-MS. The parameters were optimized for the desired mass/charge range (50-500 m/z). A Na-formate solution was injected after each sample for internal calibration (relative weight error <2 ppm). Collision-induced fragmentation (CID) was used for the MS/MS analysis of reaction products. Different collision energies were applied between 5 and 30 eV, and the optimum fragmentation energy was ca. 13 eV. Mass spectra were recorded with otofControl 4.1 and processed with Compass DataAnalysis 4.4 (200.55.2969) softwares.

Matrix rank analysis (MRA) was performed using MatLab software to determine the number of colored species taking part in the decomposition processes.

## New scientific results

**1. The rate constants for the formation of 17 *N*-chloro amino acids were determined over a wide pH range. We have shown that the pH dependence of the reaction rate is controlled by the protonation equilibria of the reactants. The chlorination reaction was confirmed to occur between HOCl and the deprotonated amino group.**

The formation of *N*-chloro amino acids from hypochlorous acid and amino acids occurs in an overall second order reaction according to equation (1).

$$\frac{dc_{\text{HOCl}}}{dt} = -k_{\text{obs}}^{2\text{nd}} c_{\text{HOCl}} c_{\text{AA}} \quad (1)$$

The stopped-flow method was used to determine the pH-dependent rate constants ( $k_{\text{obs}}^{2\text{nd}}$ ) as function of pH (Figure 1).

On the basis of the experimental results, it has clearly been demonstrated that the formation of *N*-chloro amino acids takes place between the protonated HOCl and the deprotonated amino acid from the 4 possible reaction paths.

The experimental data (Figure 1) were fitted to equation (2) in order to determine the pH independent second order rate constants ( $k$ ). The results are shown in Figure 2. The activation enthalpy and entropy were determined for the formation of *N*-chloro amino acids on the basis of temperature dependent kinetic studies. These parameters are very similar for each system indicating that the structures and the N – Cl bond strengths of the activated complexes are not affected by the substituents on the  $\alpha$ -carbon atoms of the amino acids.

$$k_{\text{obs}}^{2\text{nd}} = k \frac{K_{\text{AA}}[\text{H}^+]}{(K_{\text{AA}} + [\text{H}^+])(K_{\text{HOCl}} + [\text{H}^+])} \quad (2)$$

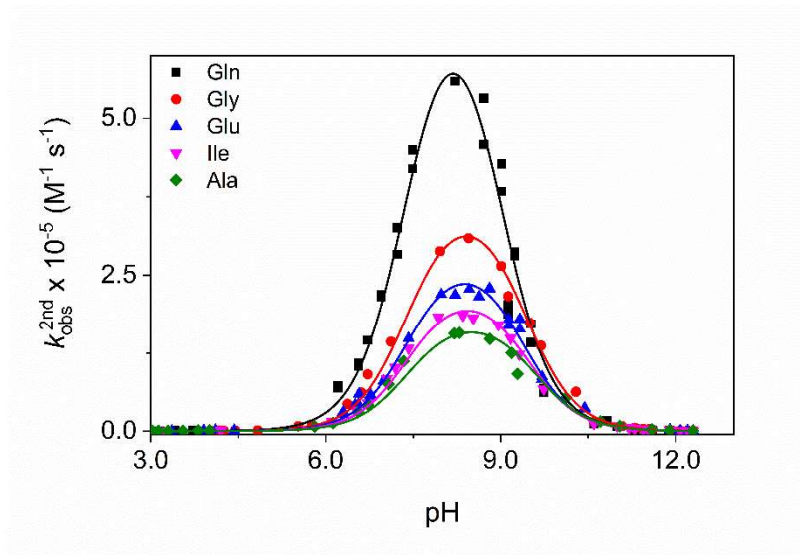


**Figure 1.** The pH dependence of  $k_{\text{obs}}^{2\text{nd}}$ . Markers: experimental data. Solid lines: fitted curves based on equation (2).

$c_{\text{NCl}} = 5.00 \times 10^{-4} \text{ M}$ ,  $c_{\text{AA}} = 7.50 \times 10^{-4} \text{ M}$ ,  $I = 1.00 \text{ M (NaClO}_4)$ ,  $T = 25.0 \text{ }^\circ\text{C}$ .

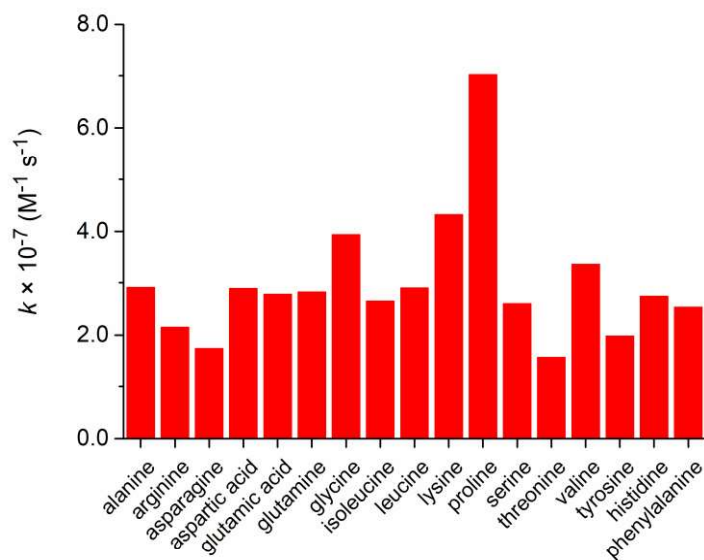


**Figure 2.** The pH independent second order rate constants of the chlorination reactions of various amino acids.

$I = 1.00 \text{ M (NaClO}_4)$ ,  $T = 25.0 \text{ }^\circ\text{C}$ .

We have shown that the chlorination of lysine is most likely to occur solely on the  $\alpha$ -amino group under physiological conditions, but the simultaneous reaction of the  $\epsilon$ -amino group cannot be excluded in alkaline medium.

**2. We proved that, with the exception of histidine, the aromatic side chain is not involved in the chlorination reaction when the amino acid is used in excess. The chlorination of histidine occurs via two pH dependent paths leading to the formation of *N*-chloramine and a product chlorinated on the side chain.**

It was confirmed that the aromatic side chain does not react with HOCl in the case of phenylalanine. According to our detailed studies, deprotonation of the OH group of the tyrosine side chain does not affect the reactivity of the amino group. The NMR spectra of the respective reaction mixtures verify that the chlorination of the aromatic rings of the side chains of tryptophan and tyrosine does not occur under the applied conditions.

NMR measurements confirmed that there are two pH-dependent parallel paths in the histidine – HOCl reaction leading to the formation of *N*-chloramine and a product chlorinated on the aromatic side chain. The pH-dependent second-order rate constants were fitted using equation (3). The pH-dependent second order rate constant and the contributions of the two paths to the overall process are shown as function of pH in Figure 3.

$$k_{\text{obs}}^{\text{2nd}} = \frac{k_1 K_{A1} [\text{H}^+]^2 + k_2 K_{A1} K_{A2} [\text{H}^+]}{(K_{A1} K_{A2} + K_{A1} [\text{H}^+] + [\text{H}^+]^2) (K_{\text{HOCl}} + [\text{H}^+])} \quad (3)$$

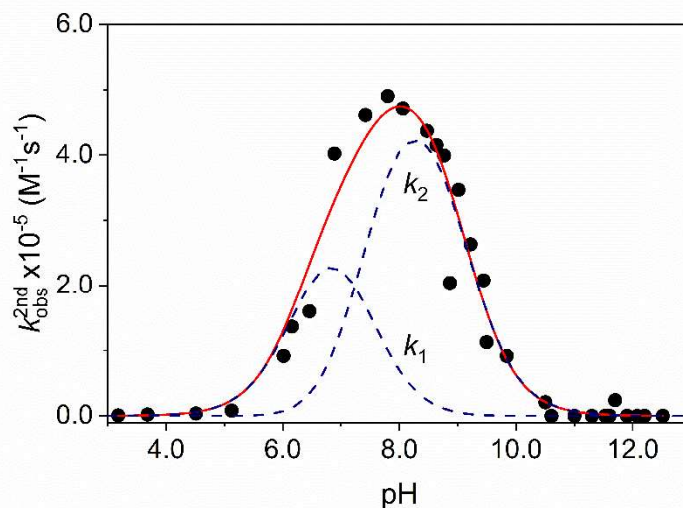


**Figure 3.** The pH dependence of the rate constant of the histidine – HOCl reaction. Markers: experimental data. Solid line: the result of fitting based on equation (3). Dashed lines: the contributions of the parallel reaction paths to the overall reaction.

$c_{\text{NCl}}^0 = 5.00 \times 10^{-4} \text{ M}$ ,  $c_{\text{AA}}^0 = 7.50 \times 10^{-4} \text{ M}$ ,  $I = 1.00 \text{ M}$  ( $\text{NaClO}_4$ ),  $T = 25.0 \text{ }^\circ\text{C}$ .

**3. It was confirmed that the decomposition of *N*-chloroglycine yields *N*-formylglycine as the main product. *N*-oxalylglycine was identified as an important intermediate in this reaction. On the basis of detailed kinetic, NMR and MS studies, a comprehensive mechanism was postulated which provides a coherent interpretation of all experimental observations.**

During the decomposition of *N*-chloroglycine (MCG), the steady decrease of the absorbance at the absorption maximum ( $\lambda_{\text{max}} = 255 \text{ nm}$ ) and at higher wavelengths corresponds to the first order decay of MCG ( $k_{\text{obs1}}$ ) (Figure 4). At lower wavelengths ( $\lambda < 240 \text{ nm}$ ), the absorbance change features a maximum as function of time (Figure 5). These observations are consistent with the formation of an intermediate which is transformed into the final product in a first order process ( $k_{\text{obs2}}$ ).

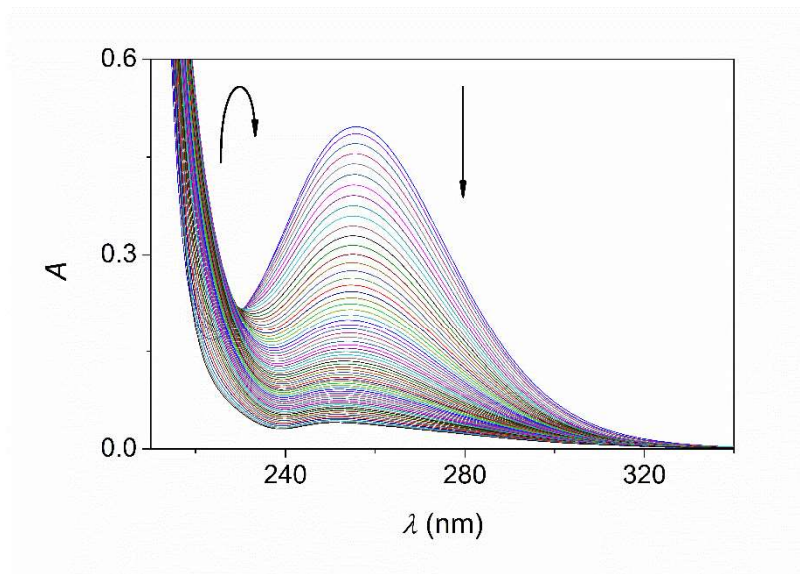


**Figure 4.** Time resolved UV-Vis spectral change after mixing hypochlorous acid and glycine.

$c_{\text{Gly}}^0 = 2.00 \times 10^{-4} \text{ M}$ ,  $c_{\text{NCl}}^0 = 1.00 \times 10^{-3} \text{ M}$ ,  $c_{\text{OH}} = 5.40 \times 10^{-2} \text{ M}$ ,  $I = 1.00 \text{ M}$  ( $\text{NaClO}_4$ ),  $T = 25.0 \text{ }^\circ\text{C}$ ,  $t = 5000 \text{ s}$ ,  $\Delta t = 40 \text{ s}$ .

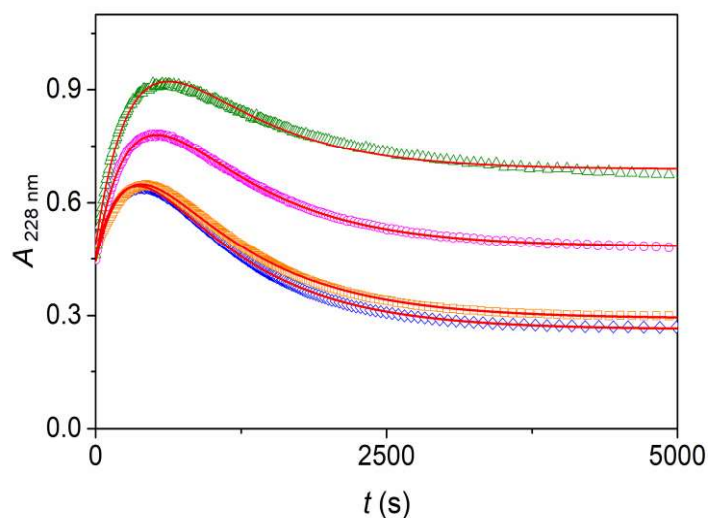


**Figure 5.** Representative kinetic curves for MCG decomposition at 280 nm (a) and at 228 nm (b) at different concentrations of excess glycine. Markers: experimental data. Solid lines: data fitting based on equation (4).

$k_{\text{obs1}} = (3.2 \pm 0.3) \times 10^{-3} \text{ s}^{-1}$ ,  $k_{\text{obs2}} = (1.2 \pm 0.1) \times 10^{-3} \text{ s}^{-1}$   
 $c_{\text{NCl}}^0 = 3.00 \times 10^{-3} \text{ M}$ ,  $c_{\text{OH}} = 5.40 \times 10^{-2} \text{ M}$ ,  $c_{\text{Gly}}^0 = 1.50 \times 10^{-3} \text{ M}$  ( $\diamond$ ),  $3.00 \times 10^{-3} \text{ M}$  ( $\square$ ),  $1.20 \times 10^{-2} \text{ M}$  ( $\circ$ ),  $2.70 \times 10^{-2} \text{ M}$  ( $\triangle$ )  $\text{M}$ ,  $I = 1.00 \text{ M}$  ( $\text{NaClO}_4$ ),  $T = 25.0 \text{ }^\circ\text{C}$ .

The rate constants of the 2 processes were estimated by fitting the kinetic curves to equation (4) at different wavelengths. It was confirmed that the second process does not contribute to the absorbance change at higher wavelengths, thus the  $k_{\text{obs}2}$  term was neglected in the corresponding calculations.

$$A = A_1 e^{-k_{\text{obs}1} t} + A_2 e^{-k_{\text{obs}2} t} + A_{\infty} \quad (4)$$

The rate of decomposition exhibits a significant dependence on pH, i.e.  $k_{\text{obs}1}$  increases linearly as function of hydroxide ion concentration. Under neutral conditions, the decomposition is extremely slow. In contrast,  $k_{\text{obs}2}$  is independent of the hydroxide ion concentration (Figure 6).

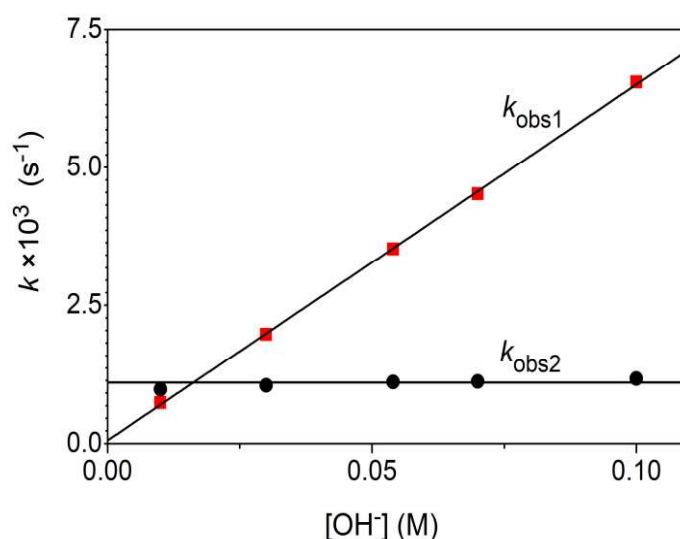


**Figure 6.** The rate constants for the decomposition of MCG as function of hydroxide ion concentration.  
 $I = 1.00 \text{ M (NaClO}_4\text{)}, T = 25.0 \text{ }^\circ\text{C}.$

The decomposition of *N*-chloroglycine was also followed by  $^1\text{H}$  and  $^{13}\text{C}$  NMR methods. It was confirmed that the major product is *N*-formylglycine. This compound forms as a mixture of *cis* and *trans* isomers in 1:9 ratio (Figure 7). *N*-oxalylglycine was identified as an intermediate. Glyoxalate ion is also an intermediate in this system and its reaction with the excess of glycine yields a

Schiff base which was clearly identified in the NMR spectra. This product is formed at a significantly lower concentration than the main product, *N*-formylglycine.

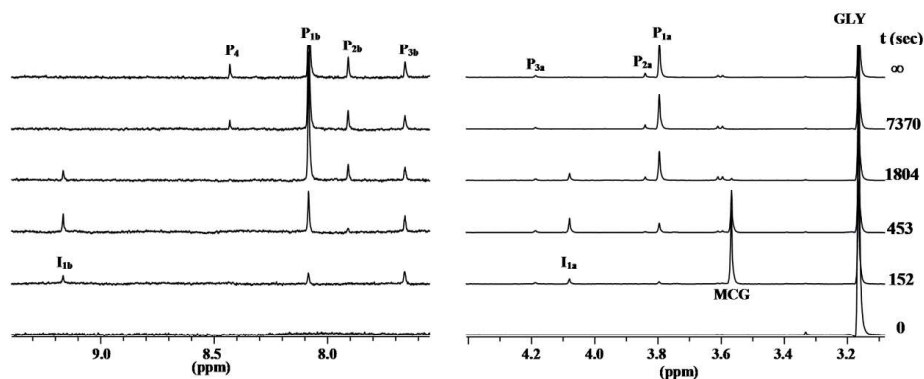


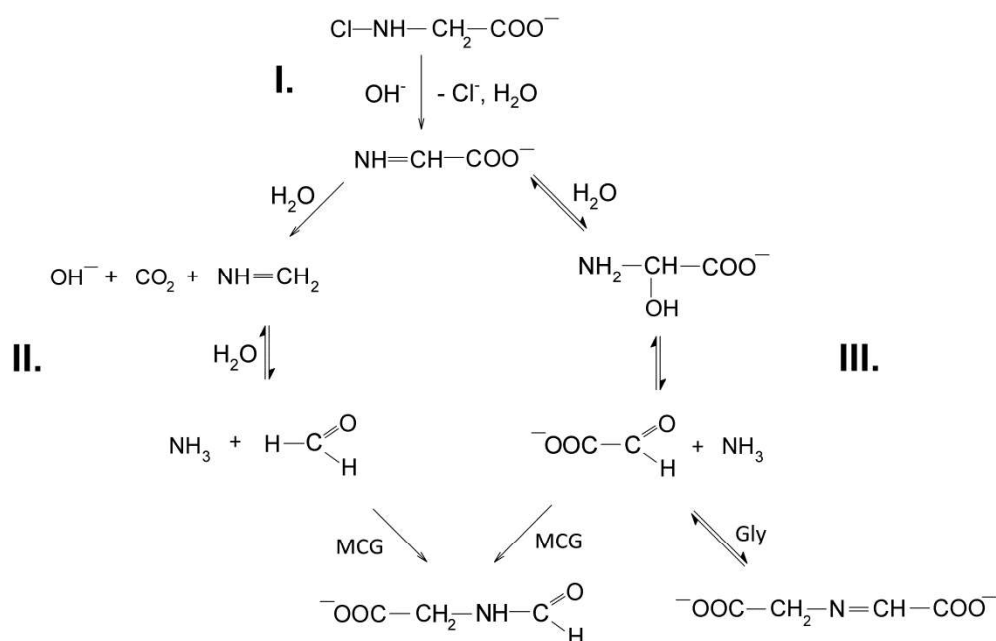
**Figure 7.** Time-dependent  $^1\text{H}$  NMR spectra during the decomposition of *N*-chloroglycine in aqueous media. The two parts of the spectra are shown in different magnifications.

MCG: *N*-chloroglycine; Gly: glycine; P1: *trans-N*-formylglycine; P2: *cis-N*-formylglycine; P3: Schiff-base; P4: formate ion.

$$c_{\text{NCl}}^0 = 1.00 \times 10^{-2} \text{ M}, c_{\text{Gly}}^0 = 1.00 \times 10^{-2} \text{ M},$$

$$c_{\text{OH}} = 5.40 \times 10^{-2} \text{ M}, T = 25.0 \text{ }^\circ\text{C}.$$

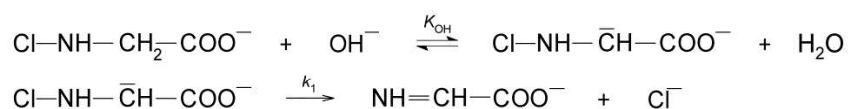
On the basis of kinetic and NMR experiments, a detailed mechanism was postulated for the decomposition of *N*-chloroglycine. The major steps of the mechanism is shown in Scheme 1.



**Scheme 1.** The outline of the decomposition mechanism of *N*-chloroglycine.

According to the proposed mechanism, the rate determining step characterized by the  $k_{\text{obs1}}$  rate constant corresponds to 2 processes. The first one is the formation of a carbanion from *N*-chloroglycine in an equilibrium deprotonation step ( $K_{\text{OH}}$ ), which is converted to iminoacetate in a subsequent irreversible reaction ( $k_1$ ) (Scheme 2).

$$k_{\text{obs1}} = K_{\text{OH}} k_1 [\text{OH}^-] \quad (5)$$



**Scheme 2.** The initial steps for the decomposition of *N*-chloroglycine as seen in Part I. of Scheme 1.

The second rate determining process ( $k_{\text{obs2}}$ ) is interpreted as the conversion of the *N*-oxalylglycine intermediate to *N*-formylglycine.

**4. It was established that the decomposition of *N*-chloroalanine takes place via 2 parallel paths that are controlled by the pH. In neutral medium, acetaldehyde is the only product of the reaction. Under alkaline conditions, pyruvate ion is the major product, but *N*-acetyl- $\alpha$ -alanine also forms. We have shown that the decomposition of *N*-chloroglycine and *N*-chloroalanine takes place by different mechanisms.**

In alkaline media, at 253 nm and higher wavelengths, the exponentially decreasing kinetic curves are associated with the decomposition of *N*-chloroalanine ( $k_{\text{obs1}}$ ), while at lower wavelengths, an additional process is also observed corresponding to the product formation ( $k_{\text{obs2}}$ ). These kinetic traces were fitted with equation (4) (Figure 8).

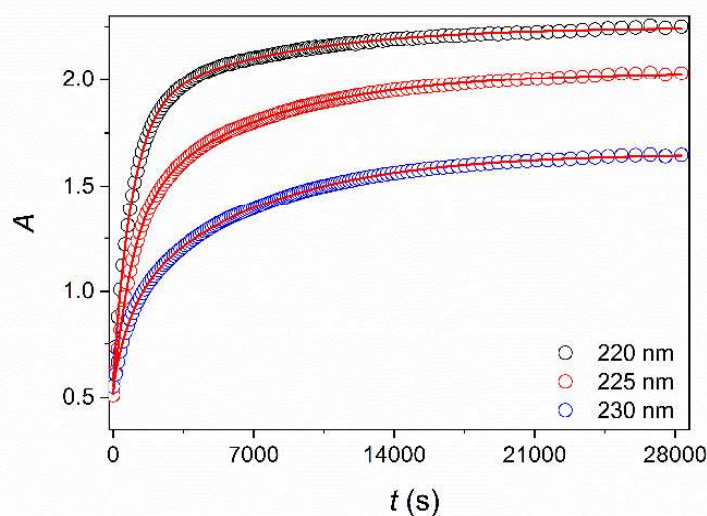


**Figure 8.** Representative kinetic traces for the decomposition of *N*-chloroalanine in alkaline media. Markers: experimental data Solid lines: fitted curves based on equation (4).

$$k_{\text{obs1}} = (1.09 \pm 0.01) \times 10^{-3} \text{ s}^{-1}, k_{\text{obs2}} = (1.46 \pm 0.02) \times 10^{-4} \text{ s}^{-1}$$

$$c_{\text{Ala}}^0 = 3.00 \times 10^{-3} \text{ M}, c_{\text{NCl}}^0 = 3.00 \times 10^{-3} \text{ M}, c_{\text{OH}^-} = 5.00 \times 10^{-2} \text{ M},$$

$$I = 1.00 \text{ M (NaClO}_4), T = 25.0 \text{ }^\circ\text{C}.$$

It was found that the spectral changes in neutral and slightly alkaline solutions are significantly different from those in strongly alkaline media. Accordingly, it is clear that the decomposition process takes place via different reaction paths depending on the pH, and the intermediates and final products are also different. It was shown that the rate constant of decomposition ( $k_{\text{obs1}}$ ) increases by increasing pH, thus the stability of the *N*-chloramine solution decreases at higher alkalinity (Figure 9).

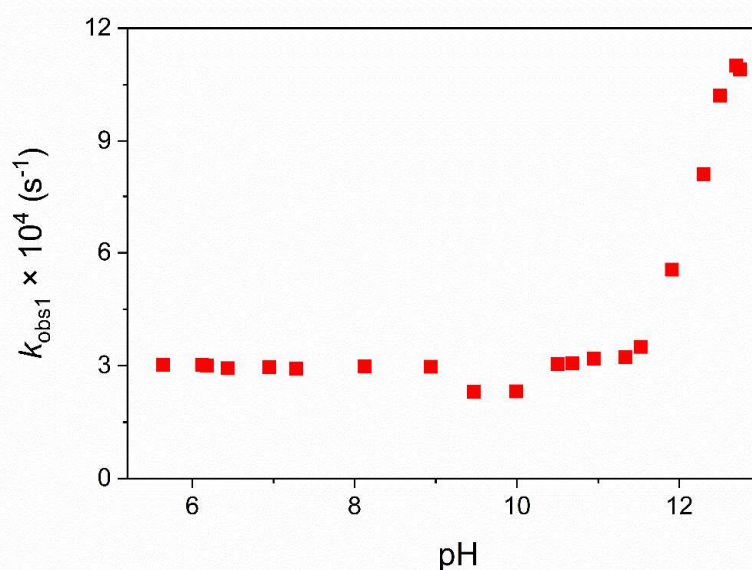


**Figure 9.** The pseudo-first order rate constant of the decomposition of *N*-chloroalanine as function of pH.

$$c_{\text{Ala}}^0 = 2.50 \times 10^{-3} \text{ M}, c_{\text{NCl}}^0 = 2.50 \times 10^{-3} \text{ M}, \\ I = 1.00 \text{ M (NaClO}_4\text{)}, T = 25.0 \text{ }^\circ\text{C}.$$

We found that the methyl side chain functional group of alanine has a significant effect on the decomposition of the *N*-chloro amino acid. The non-zero intercept of the  $k_{\text{obs1}}$  versus  $[\text{OH}^-]$  plot confirms that the decomposition of *N*-chloroalanine occurs via 2 parallel reaction paths, i.e. in a spontaneous and a hydroxide ion-catalyzed process. Accordingly, the pseudo-first order rate constant of the decomposition ( $k_{\text{obs1}}$ ) is given by equation (6), where  $k$  and  $k_{\text{OH}}$  are the rate

constants for the 2 paths. These parameters were determined by fitting the experimental data to equation (6).

$$k_{\text{obs1}} = k + k_{\text{OH}} [\text{OH}^-] \quad (6)$$

$$k = (2.95 \pm 0.09) \times 10^{-4} \text{ s}^{-1} \text{ and } k_{\text{OH}} = (1.38 \pm 0.02) \times 10^{-2} \text{ M}^{-1}\text{s}^{-1}.$$

In the case of *N*-chloroalanine, the rates of the 2 paths are comparable in the neutral – alkaline pH range. In contrast, the rate of the spontaneous decomposition of *N*-chloroglycine is negligible, as evidenced by the corresponding plot in Figure 6. This difference was interpreted by the electron-donating effect of the methyl substituent on the  $\alpha$ -carbon of  $\alpha$ -alanine.

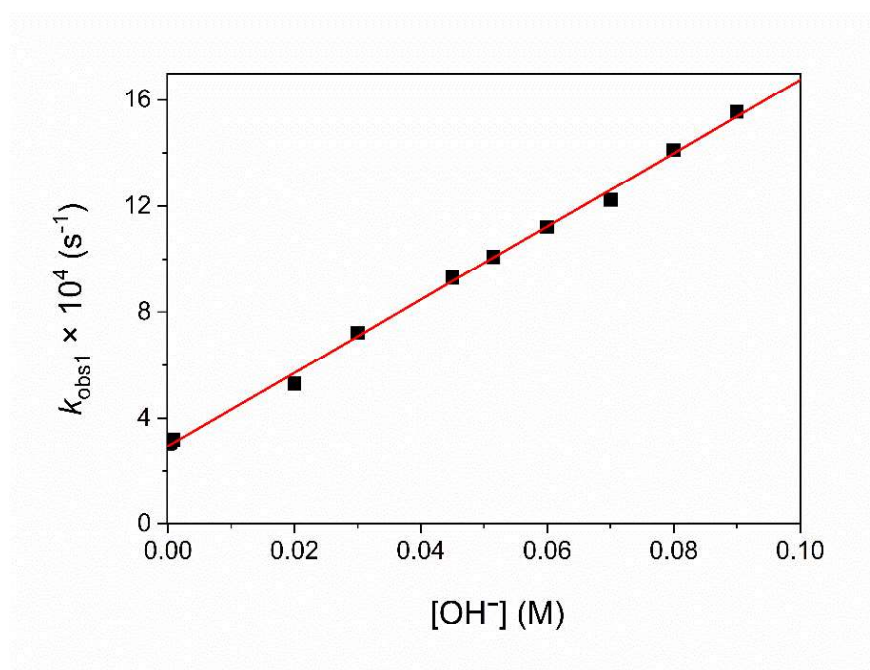


**Figure 10.** The pseudo-first order rate constant of the decomposition of *N*-chloroalanine as function of hydroxide ion concentration.  $c_{\text{Ala}}^0 = 2.50 \times 10^{-3} \text{ M}$ ,  $c_{\text{NCl}}^0 = 2.50 \times 10^{-3} \text{ M}$ ,  $I = 1.00 \text{ M}$  ( $\text{NaClO}_4$ ),  $T = 25.0 \text{ }^\circ\text{C}$ .

NMR studies have shown that pyruvate ion is the major product in the hydroxide ion catalyzed reaction. *N*-acetylalanine also forms as a by-product at low concentration level in a subsequent reaction between pyruvate ion and *N*-chloroalanine. By decreasing the pH of the reaction mixture, the concentrations of these products decrease, and acetaldehyde becomes the main product at  $\text{pH} \sim 10$  (Figure 11).

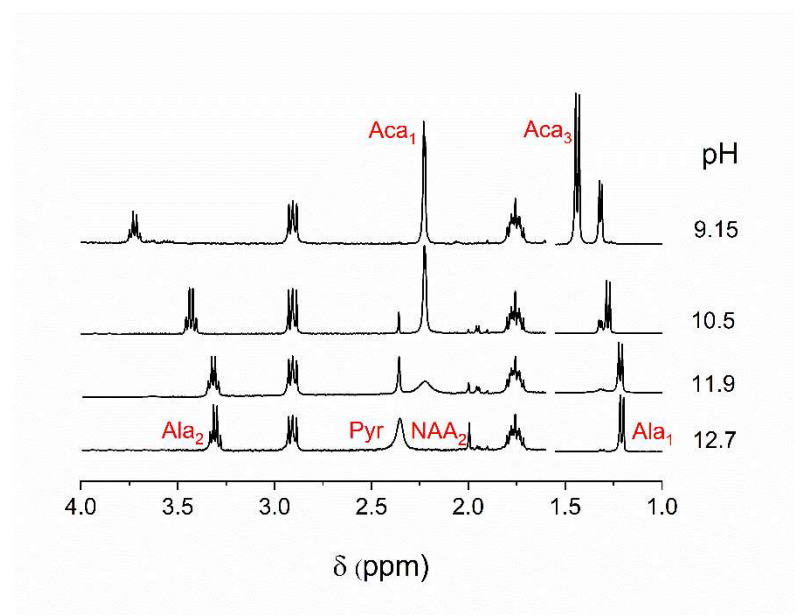


**Figure 11.** <sup>1</sup>H NMR spectra recorded at the end of the decomposition reaction of *N*-chloroalanine at various pH values.

Ala: alanine, Pyr: pyruvate ion, Aca: acetaldehyde, NAA: *N*-acetylalanine.

$$c_{\text{Ala}}^0 = 2.50 \times 10^{-3} \text{ M}, c_{\text{NCl}}^0 = 2.50 \times 10^{-3} \text{ M}, T = 25.0 \text{ } ^\circ\text{C}.$$

In contrast to assumptions in the earlier literature, we confirmed that the decomposition of *N*-chloroalanine does not occur by the one-step Grob mechanism. In accordance with the experimental results, a detailed mechanism of the decomposition reaction was postulated. The outline of this mechanism is shown in Scheme 3. Similarly to the decomposition of *N*-chloroglycine, the catalytic effect of the hydroxide ion is interpreted by the formation of a carbanion from *N*-chloroalanine.



The reaction of iminopropionate with water produces hydroxyalanine, which decomposes to pyruvate ion and ammonia. The hydration of iminopropionate is a relatively slow step followed by the rapid conversion of hydroxyalanine.

**5. It was confirmed that the decompositions of *N*-chloro branched-chain amino acids yield the corresponding aldehydes in the neutral – alkaline pH range. We explored the kinetic features of these reactions and proposed a common mechanism for the interpretation of the results. We have shown that the aldehydes are converted into the corresponding Schiff bases in reversible reactions under alkaline conditions when the amino acids are in excess.**

According to time resolved UV-Vis spectral changes during the decomposition of *N*-chloro branched-chain amino acids, *N*-chlorovaline and *N*-chloroisoleucine exhibit very similar kinetic features in the entire neutral – alkaline pH range (Figure 12). A single exponential expression fits the kinetic curves extremely well in the whole wavelength range. The pseudo-first order rate constants obtained at different wavelengths agree with each other by 1-2%.

We have shown that the spectral changes that accompany the decomposition of *N*-chloroleucine significantly differ from those observed in the decomposition of *N*-chlorovaline and *N*-chloroisoleucine under alkaline conditions (Figure 13). Similarly to the other 2 systems, the first order kinetic traces at 270 nm and higher wavelengths are consistent with the decomposition of the *N*-chloro amino acid. Spectral changes at lower wavelengths clearly show that a slow secondary reaction also occurs which is far from completion even after 12 h. We concluded that this process cannot directly be attributed to the decomposition of *N*-chloroleucine.

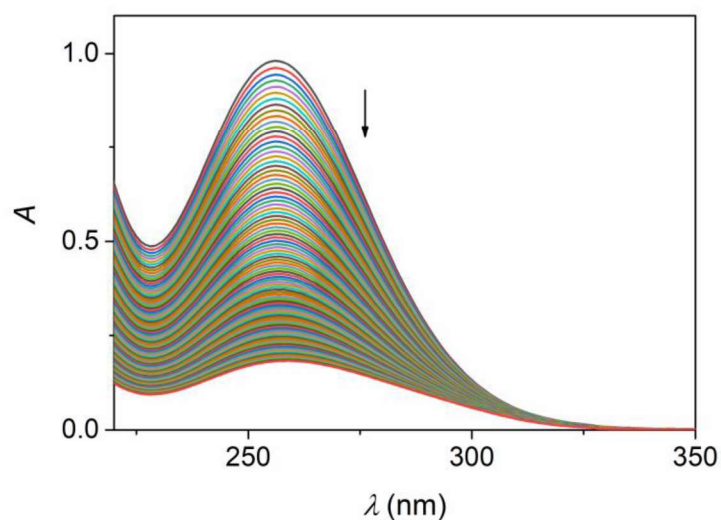


**Figure 12.** Time-dependent spectral changes that accompany the decomposition of *N*-chloroisoleucine.

$c_{\text{Ile}}^0 = 3.00 \times 10^{-3} \text{ M}$ ,  $c_{\text{NCl}}^0 = 3.00 \times 10^{-3} \text{ M}$ ,  $c_{\text{OH}^-} = 5.00 \times 10^{-2} \text{ M}$ ,  $I = 1.00 \text{ M}$  ( $\text{NaClO}_4$ ),  $T = 25.0 \text{ }^\circ\text{C}$ ,  $\Delta t = 60 \text{ s}$ ,  $t = 10800 \text{ s}$ .

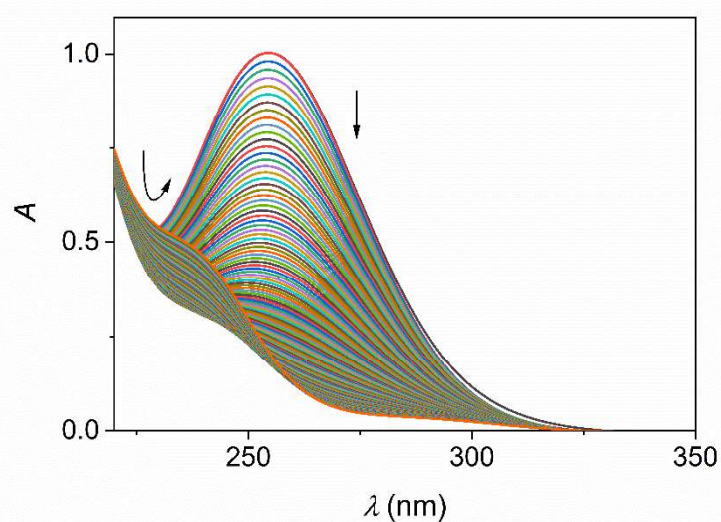


**Figure 13.** Time-dependent spectral changes that accompany the decomposition of *N*-chloroleucine.

$c_{\text{Leu}}^0 = 3.00 \times 10^{-3} \text{ M}$ ,  $c_{\text{NCl}}^0 = 3.00 \times 10^{-3} \text{ M}$ ,  $c_{\text{OH}^-} = 5.00 \times 10^{-2} \text{ M}$ ,  $I = 1.00 \text{ M}$  ( $\text{NaClO}_4$ ),  $T = 25.0 \text{ }^\circ\text{C}$ ,  $\Delta t = 60 \text{ s}$ ,  $t = 10800 \text{ s}$ .

As shown in Figure 14, the pseudo first order rate constant of the decomposition of *N*-chloro branched-chain amino acids ( $k_{\text{obs}}$ ) is a linear function of  $[\text{OH}^-]$  (equation (6)). This is similar to the case of *N*-chloroglycine and *N*-chloroalanine. The fitted straight lines in Figure 14 have non-zero intercepts, meaning that these reactions are analogous to the decomposition of *N*-chloroalanine in that they proceed via 2 competing reaction paths.

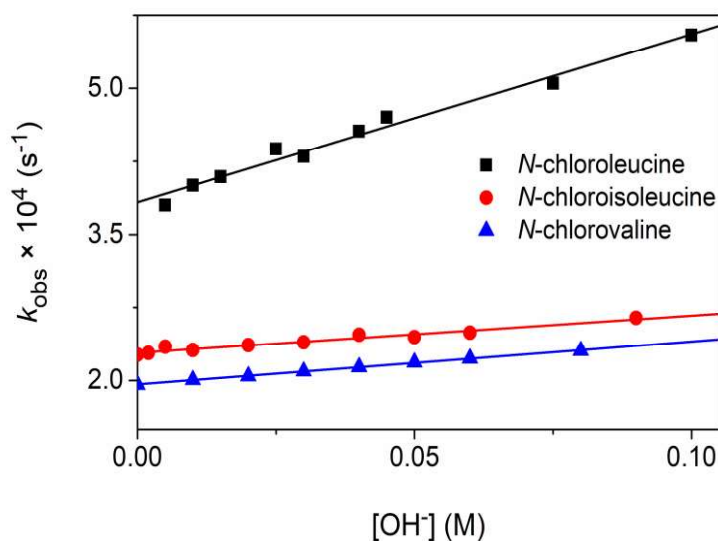
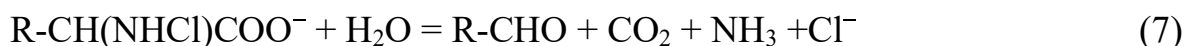


**Figure 14.** The pseudo-first order rate constants of the decompositions of *N*-chloro amino acids as function of hydroxide ion concentration.

$c_{\text{AA}}^0 = 3.00 \times 10^{-3} \text{ M}$ ,  $c_{\text{NCl}}^0 = 3.00 \times 10^{-3} \text{ M}$ ,  $I = 1.00 \text{ M}$  ( $\text{NaClO}_4$ ),  $T = 25.0 \text{ }^\circ\text{C}$ .

It was also confirmed that the reactivity of *N*-chloroisoleucine and *N*-chlorovaline is very similar, but the decomposition of *N*-chloroleucine is approximately twice and four times faster via the pH-independent and  $[\text{OH}^-]$ -dependent paths, respectively.

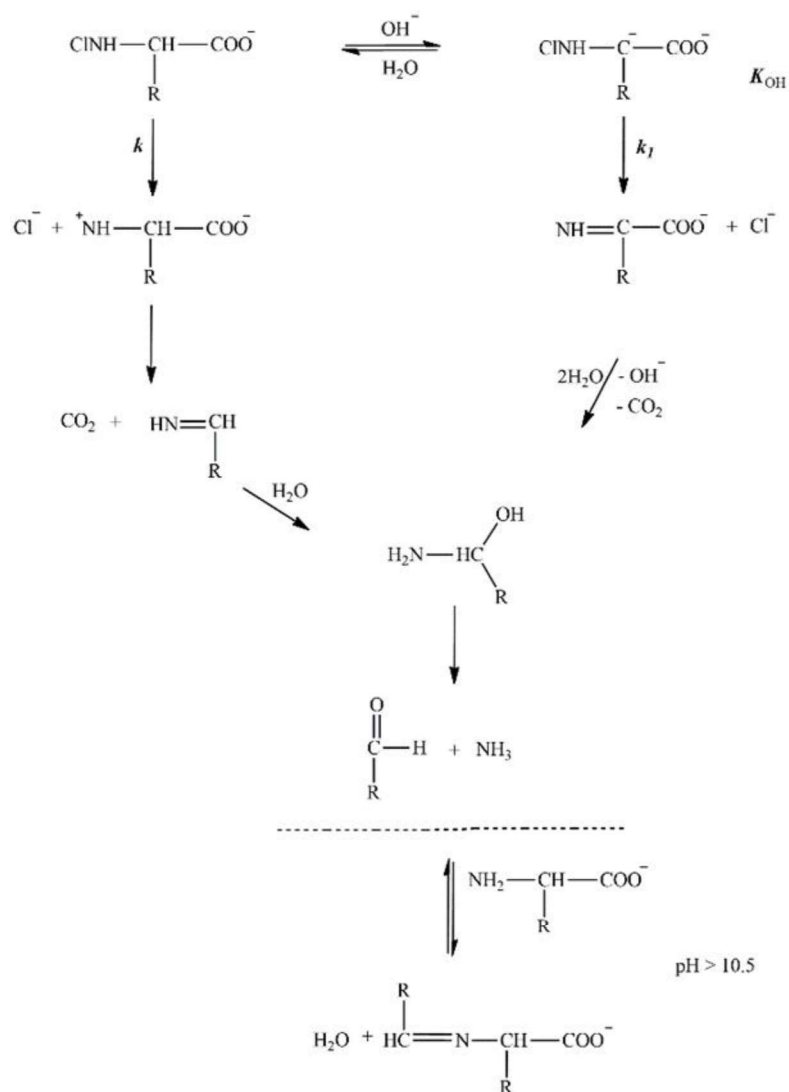
In the decomposition of each *N*-chloro branched-chain amino acid, the formation of the corresponding aldehyde was observed, and the overall process is described by equation (7).



By increasing the pH, new peaks were identified in the NMR spectra. These confirmed the formation of the corresponding Schiff base in a reversible reaction between the aldehyde and the excess amino acid. As the amino acid concentration increases, the intensity of the Schiff base signal increases continuously, even when the concentration ratio of amino acid to aldehyde is greater than 1: 1. This indicates that only a part of the aldehyde is converted into a Schiff base under these conditions.

The decompositions of the chloramines of branched-chain amino acids show different features compared to the decompositions of the chloramines of glycine and alanine. In the decomposition of the latter compounds, 2 successive rate-determining steps are operative via the hydroxide ion-catalyzed path. The second step was interpreted by considering the reactions between reactive intermediates and *N*-chloro amino acids. Such a process does not take place during the decomposition of *N*-chloroleucine, -isoleucine and -valine. Experimental results show that the same aldehyde is formed via the pH-independent and the [OH<sup>-</sup>]-dependent paths. This is an unexpected result, especially by considering that different products form during the decomposition of *N*-chloroalanine under neutral and strongly alkaline conditions.

Similarly to the systems discussed in the previous chapters, the [OH<sup>-</sup>] dependency of the pseudo first order rate constants of the decompositions of the *N*-chloro branched-chain amino acids ( $k_{\text{obs}}$ ) are also consistent with the formation of carbanions in fast equilibrium steps with OH<sup>-</sup>. These are followed by the rate determining steps ( $k_1$ ). In the case of *N*-chloroalanine, deamination of the imine leads to the stabilization of the 2-keto-carboxylic acid product. This reaction step can be ruled out for the chloramines discussed in this chapter, because decarboxylation must precede the deamination to give the aldehyde as the final product. It is hypothesized that the presence of a relatively large alkyl side chain results in the release of CO<sub>2</sub> instead of NH<sub>3</sub> (Scheme 4). This sequence leads to the formation of the same hemiaminal as the pH-independent path does.



**Scheme 4.** General mechanism of the decompositions of chloramines formed from branched-chain amino acids.

## **Possible utilization of the results**

We extensively studied the kinetics and mechanism of the chlorination reactions between hypochlorous acid and different amino acids. The details of the formation and decomposition kinetics of *N*-chloro amino acids formed in these processes have been described. We have confirmed the formation of various intermediates and end products, and estimated their concentrations and concentration ratios. This may contribute to the identification of compounds that form during water treatment technologies. Some of these compounds can cause taste and odor issues in drinking water. Their presence may also induce health problems associated with the consumption of treated water. Our results may contribute to optimizing water treatment processes and producing higher quality drinking water.

The reactions studied have significant biological roles, as well, because they occur in living organisms. Thus, the elucidation of the detailed mechanism of these reactions is biologically important and contributes to a deeper understanding of *in vivo* processes. Many of the identified intermediates and products are actively involved in various biological processes, for example, by affecting the functions of enzymes. Thus, our results also help to understand the molecular background of the biological effects attributed to the *in vivo* decomposition of *N*-chloro amino acids.



Registry number: DEENK/308/2019.PL  
Subject: PhD Publikációs Lista

Candidate: Mária Szabó  
Neptun ID: DYWHQD  
Doctoral School: Doctoral School of Chemistry  
MTMT ID: 10051172

### List of publications related to the dissertation

#### Foreign language scientific articles in international journals (5)

1. **Szabó, M.**, Bíró, V., Simon, F., Fábán, I.: The decomposition of N-chloro amino acids of essential branched-chain amino acids: kinetics and mechanism.  
*J. Hazard. Mater.* 382, 1-8, 2020. ISSN: 0304-3894.  
DOI: <http://dx.doi.org/10.1016/j.jhazmat.2019.120988>  
IF: 7.65 (2018)
2. Simon, F., **Szabó, M.**, Fábán, I.: pH controlled byproduct formation in aqueous decomposition of N-chloro- $\alpha$ -alanine.  
*J. Hazard. Mater.* 362, 286-293, 2019. ISSN: 0304-3894.  
DOI: <http://dx.doi.org/10.1016/j.jhazmat.2018.09.004>  
IF: 7.65 (2018)
3. **Szabó, M.**, Simon, F., Fábán, I.: The formation of N-chloramines with proteinogenic amino acids.  
*Water Res.* 165, 1-8, 2019. ISSN: 0043-1354.  
DOI: <http://dx.doi.org/10.1016/j.watres.2019.114994>  
IF: 7.913 (2018)
4. **Szabó, M.**, Bellér, G., Kalmár, J., Fábán, I.: The Kinetics and Mechanism of Complex Redox Reactions in Aqueous Solution: The Tools of the Trade.  
*Adv. Inorg. Chem.* 70, 1-61, 2017. ISSN: 0898-8838.  
DOI: <http://dx.doi.org/10.1016/bs.adioch.2017.02.004>  
IF: 1.316
5. **Szabó, M.**, Baranyai, Z., Somsák, L., Fábán, I.: Decomposition of N-Chloroglycine in Alkaline Aqueous Solution: Kinetics and Mechanism.  
*Chem. Res. Toxicol.* 28 (6), 1282-1291, 2015. ISSN: 0893-228X.  
DOI: <http://dx.doi.org/10.1021/acs.chemrestox.5b00084>  
IF: 3.025





## List of other publications

### Foreign language scientific articles in international journals (5)

6. Gáspár, A., Pesti, A., **Szabó, M.**, Kecskeméti, Á.: Determination of chlorine species by capillary electrophoresis: mass spectrometry.  
*Electrophoresis. Epub*, 1-8, 2019. ISSN: 0173-0835.  
DOI: <http://dx.doi.org/10.1002/elps.201900138>  
IF: 2.754 (2018)
7. **Szabó, M.**, Kalmár, J., Ditroi, T., Bellér, G., Lente, G., Simic, N., Fábíán, I.: Equilibria and kinetics of chromium(VI) speciation in aqueous solution ? A comprehensive study from pH 2 to 11.  
*Inorg. Chim. Acta.* 472, 295-301, 2018. ISSN: 0020-1693.  
DOI: <http://dx.doi.org/10.1016/j.ica.2017.05.038>  
IF: 2.433
8. Kalmár, J., **Szabó, M.**, Simic, N., Fábíán, I.: Kinetics and mechanism of the chromium(IV) catalyzed decomposition of hypochlorous acid at elevated temperature and high ionic strength.  
*Dalton Trans.* 47 (11), 3831-3840, 2018. ISSN: 1477-9226.  
DOI: <http://dx.doi.org/10.1039/C8DT00120K>  
IF: 4.052
9. Najóczki, F., Bellér, G., **Szabó, M.**, Fábíán, I.: Substituent effect on the N-oxidation of 1,10-phenanthroline derivatives by peroxomonosulfate ion.  
*New J. Chem.* 41 (18), 9947-9953, 2017. ISSN: 1144-0546.  
DOI: <http://dx.doi.org/10.1039/C7NJ01860F>  
IF: 3.201
10. Bellér, G., **Szabó, M.**, Lente, G., Fábíán, I.: Formation of 1,10-Phenanthroline-N,N'-dioxide under Mild Conditions: The Kinetics and Mechanism of the Oxidation of 1,10-Phenanthroline by Peroxomonosulfate Ion (Oxone).  
*J. Org. Chem.* 81 (13), 5345-5353, 2016. ISSN: 0022-3263.  
DOI: <http://dx.doi.org/10.1021/acs.joc.6b00641>  
IF: 4.849

**Total IF of journals (all publications): 44,843**

**Total IF of journals (publications related to the dissertation): 27,554**

The Candidate's publication data submitted to the iDEa Tudóstér have been validated by DEENK on the basis of the Journal Citation Report (Impact Factor) database.

03 September, 2019

